Chemosphere 226 (2019) 687–695

Contents lists available at ScienceDirect

Chemosphere

journal homepage: www.elsevier.com/locate/chemosphere

Al_2O_3 nanoparticles promote secretion of antibiotics in *Streptomyces coelicolor* by regulating gene expression through the nano effect

Xiaomei Liu [a], Jingchun Tang [a, *], Lan Wang [a], John P. Giesy [b, c]

[a] Key Laboratory of Pollution Processes and Environmental Criteria (Ministry of Education), Tianjin Engineering Research Center of Environmental Diagnosis and Contamination Remediation, College of Environmental Science and Engineering, Nankai University, Tianjin, 300350, China
[b] Toxicology Centre, University of Saskatchewan, Saskatoon, Saskatchewan, Canada
[c] Department of Veterinary Biomedical Sciences, University of Saskatchewan, Saskatoon, Saskatchewan, Canada

HIGHLIGHTS

- It is the first report NPs had effects on antibiotic production of *S. coelicolor*.
- 1000 mg/L Al_2O_3 NPs resulted in 3.7 and 4.6-fold enhance production of RED and ACT.
- Al_2O_3 NPs could increase the expression levels of antibiotic biosynthetic genes.
- Effects of NPs on antibiotic secretion are attributed by the nano effect.

GRAPHICAL ABSTRACT

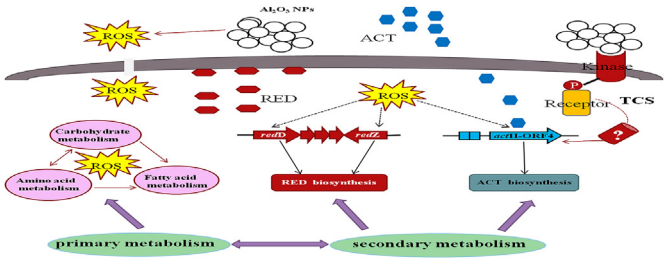

ARTICLE INFO

Article history:
Received 15 December 2018
Received in revised form
12 March 2019
Accepted 25 March 2019
Available online 28 March 2019

Handling Editor: Tamara S. Galloway

Keywords:
Al_2O_3 NPs
ROS
Streptomyces coelicolor M145
Antibiotic production
Transcriptome

ABSTRACT

Toxic effects of nanoparticles (NPs) on microorganisms have attracted substantial attention; however, there are few reports on whether NPs can affect the secondary metabolism of microbes. To investigate the toxic effects of Al_2O_3 NPs on cell growth and antibiotic secretion, *Streptomyces coelicolor* M145 was exposed to Al_2O_3 NPs with diameters of 30 and 80 nm and bulk Al_2O_3 at concentrations up to 1000 mg/L. The results indicated that differences in the toxicity of Al_2O_3 NPs were related to the particle size. In treatment with Al_2O_3 NPs, the maximum yields of undecylprodigiosin (RED) and actinorhodin (ACT) were 3.7- and 4.6-fold greater than that of the control, respectively, and the initial time of antibiotic production was much shorter. ROS quenching experiment by N-acetylcysteine (NAC) confirmed that ROS were responsible for the increased RED production. From 0 to 72 h, ROS had a significant impact on ACT production; however, after 72 h, the ROS content began to decrease until it disappeared. During ongoing exposure (0–144 h), ACT production continued to increase, indicating that in addition to ROS, nano effect of Al_2O_3 NPs also played roles in this process. Transcriptional analysis demonstrated that Al_2O_3 NPs could increase the expression levels of antibiotic biosynthetic genes and two-component systems (TCSs) and inhibit the expression levels of primary metabolic pathways. This study provides a new perspective for understanding the mechanisms of antibiotic production in nature and reveals important implications for exploring other uses of NPs in biomedical applications or regulation of antibiotics in nature.

1. Introduction

Because physical and chemical properties of nano particles (NPs) vary significantly from their bulk counterparts (Robichaud

* Corresponding author.
E-mail address: tangjch@nankai.edu.cn (J. Tang).

https://doi.org/10.1016/j.chemosphere.2019.03.156
0045-6535/

et al. 2009; Oberdorster and Oberdorster, 2005), and due to their unique antimicrobial, electronic, optical and structural strength enhancement properties, there has been an increase in the use of nanoparticles in many applications (Balazs et al. 2006; Dinesh et al. 2012; Lee et al. 2010). Among NPs, aluminum oxide (Al_2O_3) NPs are one of the most commonly used varieties, which are widely used in absorbent material, antibacterial materials and abrasive materials (Bhatnagar et al. 2010; Ganguly and Poole, 2003; Martınez-Flores et al. 2003; Sadiq et al. 2009).

Increasing usage of NPs will inevitably lead to their release into the environment and necessitates a basic understanding of their interactions with natural biological processes, which could cause risks to ecosystems (Eduok et al. 2013; Schaumann et al. 2015). Al_2O_3 NPs are toxic to various gram-positive and gram-negative bacteria (Jiang et al. 2009), which could induce the generation of reactive oxygen species (ROS) and cause cell membrane damage (Ding et al. 2016; Qiu et al. 2012; Simon-Deckers et al. 2009). A possible mechanism by which Al_2O_3 NPs attached to bacterial surfaces might be via electrostatic interactions (Kaweeteerawat et al. 2015; Mu et al. 2015). FT-IR analyses and Zeta potentials analysis indicated that the surface charge-based attachment of nanoparticles to bacterial cell walls should be responsible for their toxicity (Kamnev, 2008; Pakrashi et al. 2011).

Streptomyces, a kind of Actinobacterium, are widely distributed in soil, accounting for 5–30% of the total soil microorganisms, and play an important role in mineralization of complex organic matters. *Streptomyces* have complex life cycles, undergoing differentiation from spore to substrate mycelia, aerial mycelia, spore chains, and mature spore (Bentley et al., 2002). More importantly, they can produce two-thirds of the clinically used antibiotics of natural origin. *S. coelicolor* is the best-known representative of the *Streptomyces* genus, and it has a 8.7-Mb genome that codes for more than 20 gene clusters whose gene products are involved in the biosynthesis of secondary metabolites as antibiotics (Borodina et al. 2008). Two of these secondary metabolites are pigmented. One is a diffusible, blue pigment called actinorhodin (ACT), and the other is undecylprodigiosin (RED), a red pigment associated with the cell wall (Cerdeño et al. 2001; Gottelt et al. 2010; Kim et al. 2016). ACT inhibits the growth of gram-positive bacteria (Xu et al. 2012) and was the first antibiotic whose entire biosynthetic gene cluster was cloned (Taguchi et al. 2013); furthermore, ACT related genes have served as an excellent model system for studying antibiotic biosynthesis and regulation. RED has antimicrobial activities and immunosuppressive and anticancer properties (Papireddy et al. 2011; Williamson et al. 2006). Antibiotic production of *S. coelicolor* is controlled by many factors, such as metabolic and nutritional status and transcriptional regulators (van Wezel et al. 2000; Yang et al. 2005), and it has been proposed that there is a coupling between antibiotic synthesis and antibiotic regulatory protein (Hindra et al. 2010). These regulatory mechanisms can be altered by varying culture conditions and changing various factors (Schäberle et al. 2014). However, there are few reports on whether nanomaterials could affect antibiotic production.

In this study, various concentrations of Al_2O_3 with different particle sizes were applied during the fermentation period of *S. coelicolor*. Subsequently, toxicity assays were performed to determine the effects of Al_2O_3 NPs on cell viability, and antibiotic secretion. To explore the mechanisms of how Al_2O_3 NPs affected antibiotic production, transcriptome analysis was carried out on the expression of *S. coelicolor* genome after exposure to Al_2O_3 NPs or not. To the best of our knowledge, this is the first report to show that Al_2O_3 NPs have a significant effect on antibiotic secretion.

2. Materials and methods

2.1. Characterization of Al_2O_3 particles

The α-Al_2O_3 NPs with particle size of 30 nm and 80 nm and bulk particles (BPs) was purchased from Shanghai Macklin Biochemical company (Shanghai, China). The morphologies and sizes of the three kinds of Al_2O_3 particles were determined via a scanning electron microscope (SEM, JEOL, Beijing, China). The particles were added to YBP medium (yeast extract: 2 g/L, beef extract powder: 2 g/L, peptone: 4 g/L, NaCl: 15 g/L, glucose: 10 g/L, $MgCl_2$: 1 g/L), which was then sonicated (100 W, 40 kHz) for 30 min to facilitate dispersion. The sizes of the particles and agglomerates in solution were measured by dynamic light scattering (DLS) with a Zetasizer nano ZS (Malvern, Worcestershire, UK). The data were collected in triplicate at 25 °C.

2.2. Bacterial culture

S. coelicolor M145 was purchased from the China General Microbiological Culture Collection Center (Beijing, China) and was cultivated on mannitol soy (MS) plates for 7 days at 30 °C. The spores were harvested, suspended in 20% (v/v) glycerol and stored at −80 °C (Li et al. 2016; Sigle et al. 2016). Fermentation cultures of M145 were prepared by inoculating 300 μL (10^8 cfu/mL) of the spore suspension into a shaking flask with 100 mL of sterilized YBP medium. The cultures were incubated on an orbital shaker at 30 °C.

2.3. Cell viability staining and confocal laser scanning microscopy

The cytotoxicity of Al_2O_3 NPs to M145 was assessed by measuring changes in the relative abundances of viable cells bacteria with the LIVE/DEAD Bac-Light bacterial viability kit (L-13152, Invitrogen, USA) after being cultured for 48 h in YBP medium with various amounts of Al_2O_3 NPs (Liu et al. 2018). Two kinds of fluorescent nucleic acid stains, SYTO 9 and propidium iodide (PI) were used to distinguish bacteria with intact cell membranes from bacteria with damaged membranes (Binh et al. 2014). The fluorescence intensity was measured by a microplate reader (Synergy H4, BioTek, Vermont, America) with fluorescence wavelengths of green (excitation 485 nm and emission 530 nm) and red (excitation 485 nm and emission 630 nm). The relative abundances of viable bacterial cells in each well were calculated with the method previously described (Liu et al. 2018). The fluorescence images were obtained with a confocal laser scanning microscope (CLSM, LSM880 with Airyscan, Zeiss, German) with the same wavelengths as the microplate reader.

2.4. Intracellular reactive oxygen species (ROS)

To measure the ROS levels, the cell permeable reagent of 2′,7′-dichlorofluorescein diacetate (DCFH-DA) (Beyotime, China) was used as a fluorescent probe to measure the intracellular ROS concentration. Briefly, after exposure to 30 nm, 80 nm and bulk particles of 0, 10, 50,100, 500 and 1000 mg/L for 48 h, the cells were centrifuged and washed three times with 0.9% NaCl. They were then suspended in 0.1 M phosphate buffer (PBS, pH 7.2) with 10 μmol/L DCFH-DA and incubated in the dark at 30 °C for 30 min, followed by washing three times with 0.9% NaCl. The fluorescence intensity was measured by a microplate reader with an excitation wavelength of 485 nm and an emission wavelength of 530 nm. The relative ROS level was represented as the fluorescence intensity ratio of the exposure group to the control group with the same dry mass (Liu et al. 2018).

2.5. ROS elimination analysis

M145 was cultured in two media, pure YBP medium as the control and YBP with Al_2O_3 NPs (80 nm, 1000 mg/L), with shaking at 30 °C. 2 mM N-acetylcysteine (NAC, an ROS scavenger) (Ding et al. 2016), was then added to the medium one hour before Al_2O_3 NPs was added. Every treatment was conducted in triplicate, and the ROS concentrations, mortality, the concentrations of the two antibiotics and the expression levels of pathway-specific regulatory genes (*actII-ORF4*, *redD*) were measured.

2.6. Extraction and quantification of antibiotics

Aliquots of 10 mL of culture medium were removed at intervals of 24 h. To estimate dry mass of the M145, 5 mL samples were washed three times with 0.9% NaCl and collected on a preweighed filter by vacuum; subsequently, the filters containing the mycelium were freeze-dried and the mass was determined (Hesketh et al. 2007; Huang et al. 2015). To estimate the antibiotic concentrations, another 5 mL of the culture was centrifuged at 4000 $\times g$ for 10 min. The supernatant from the cells was separated, to which an equal volume of 1 M NaOH was added. The mixture was then centrifuged at 4000 $\times g$ for 5 min after incubation for one hour at room temperature. Finally, the value of the absorbance at 633 nm was measured with an ultraviolet spectrophotometer to quantify the ACT abundance (T6, Persee, Beijing, China) (Bhatia et al. 2016). RED is an intracellular red pigment that must be extracted from the cell pellet before measurement. Therefore, the cells were suspended in 5 mL of methanol (adjusted to a pH of 2 beforehand with 0.1 M HCl) and incubated at 37 °C with shaking at 150 rpm overnight. Cells were then removed by centrifugation at 4000 $\times g$ for 5 min, and the RED concentrations were determined by measuring the absorbance at 533 nm (Bhatia et al. 2016). The concentrations of the antibiotics were calculated from molar extinction coefficients of 100,500 and 25,320 per cm path-length for RED and ACT, respectively (Patkari and Mehra, 2013).

2.7. Transcriptome sequencing and gene expression analyses

M145 was cultured in two types of media, pure YBP medium as the control and YBP with Al_2O_3 NPs (80 nm, 1000 mg/L), with shaking at 30 °C for 20 h. Samples were then collected by centrifugation and ground into powder in liquid nitrogen. RNA isolations were performed with Trizol (Invitrogen, Carlsbad, USA) according to procedures recommended by the manufacturer. RNA purification, cDNA synthesis, DNA library construction, sequencing and data analyses of the transcriptome were performed by the Gene Denovo Biotechnology Co. (Guangzhou, China) with an Illumina HiSeq™ 2500 instrument.

2.8. Statistical analysis

Data were expressed as the mean ± SD and analyzed with the IMB SPSS statistics 22 statistical software. Significant differences were assessed with one-way ANOVA with the Student-Newman-Keuls test (S-N-K test), and $p < 0.05$ was considered statistically significant. Each experiment was performed independently at least three times.

3. Results and discussion

3.1. Characterization of the Al_2O_3 particles

Based on the SEM images of various sizes of Al_2O_3 particles (Fig. S1), the diameters were consistent with those specified by the manufacturer. The particles were ellipsoidal in shape. The distributions of the various sizes in the YBP medium were measured by DLS analysis, which showed that the aggregated size of the NPs was between 827 and 912 nm, and for the BPs, there was no significant difference in size between the powdered particles and those in solution (Table S2). The different aggregate sizes in the media might underlie the various effects of NPs and BPs on M145.

3.2. Toxic effects of different size of Al_2O_3 particles on S. coelicolor M145

To verify whether Al_2O_3 particles were toxic to M145, a series of indicators were examined, including bacterial cell viability, ROS concentration and mycelia morphology. Exposure to 100 or 1000 mg/L of Al_2O_3 NPs resulted in significant differences ($p < 0.05$) in the viability of cells exposed to both 30 or 80 nm Al_2O_3 particles (Fig. 1a). In addition, the survival rate of M145 cells exposed to 80 nm Al_2O_3 NPs was greater than that of cells exposed to 30 nm NPs. These results indicated that the toxicity of Al_2O_3 NPs was related to particle size, with larger particles being less toxic. Compared with NPs, the toxic potency of BPs to M145 was much lower. Even concentrations of BPs as high as 1000 mg/L resulted in survival rates of 80%, while the survival of M145 cells exposed to the same concentration of NPs was only 20–35%.

Excessive production of ROS induced by nano particles could cause oxidative stress leading to bacterial inactivation. ROS concentrations were proportional to the concentrations of Al_2O_3 particles (Fig. 1b). When the concentrations were greater than 100 mg/L, there were significant differences ($p < 0.05$) in the concentrations of ROS in the cells exposed to Al_2O_3 of varying sizes (30 nm, 80 nm or BPs), which were inversely proportional to the size of the particles. When the concentration of the NPs reached 1000 mg/L, the ROS concentration was 5- to 6-fold greater than that of the controls. For BPs, even when exposed to 1000 mg/L Al_2O_3, the ROS concentrations increased only slightly.

To further test the hypothesis that the toxicity of Al_2O_3 NPs was related to particle size, CLSM was performed to visualize the bacteria after staining with SYTO 9 and PI (Fig. 1c). Different with common bacteria, *Streptomyces* can form mycelia with thousands of cells. In the absence of NPs, CK (control) showed that the mycelia were regular spheres and that most of them emitted green fluorescence. After exposure to NPs, the mycelia size decreased and were more irregular, and red fluorescence became dominant at higher NP concentrations. These results indicated that the toxicity of Al_2O_3 NPs to M145 was related to both size and concentration.

3.3. Effects of Al_2O_3 particle size on antibiotic production by S. coelicolor M145

After 21 h of culturing, control M145 did not produce any antibiotics, while RED was observed in cells exposed to 1000 mg/L Al_2O_3 NPs (80 nm) with an $OD_{533} = 0.13$ (Fig. S2a). After 48 h, this treatment was also the first to produce ACT, with an $OD_{633} = 0.28$ (Fig. S2b). These results suggested that exposure to Al_2O_3 NPs promoted production of antibiotics by M145.

To further study the effects of various sizes and concentrations of Al_2O_3 NPs on antibiotic production, a set of exposure experiments (with the relevant controls) were performed. RED is a type of intracellular antibiotic that cannot be secreted; therefore, it gradually degraded as the cells died. On the other hand, ACT is secreted after being produced and gradually accumulated in solution. The maximum RED concentration obtained in the control was approximately 1.0 mg/L (Fig. 2a). Antibiotic production was proportional to the Al_2O_3 NP concentration. When cells were exposed to 1000 mg/L and 80 nm Al_2O_3 NPs, the maximum RED

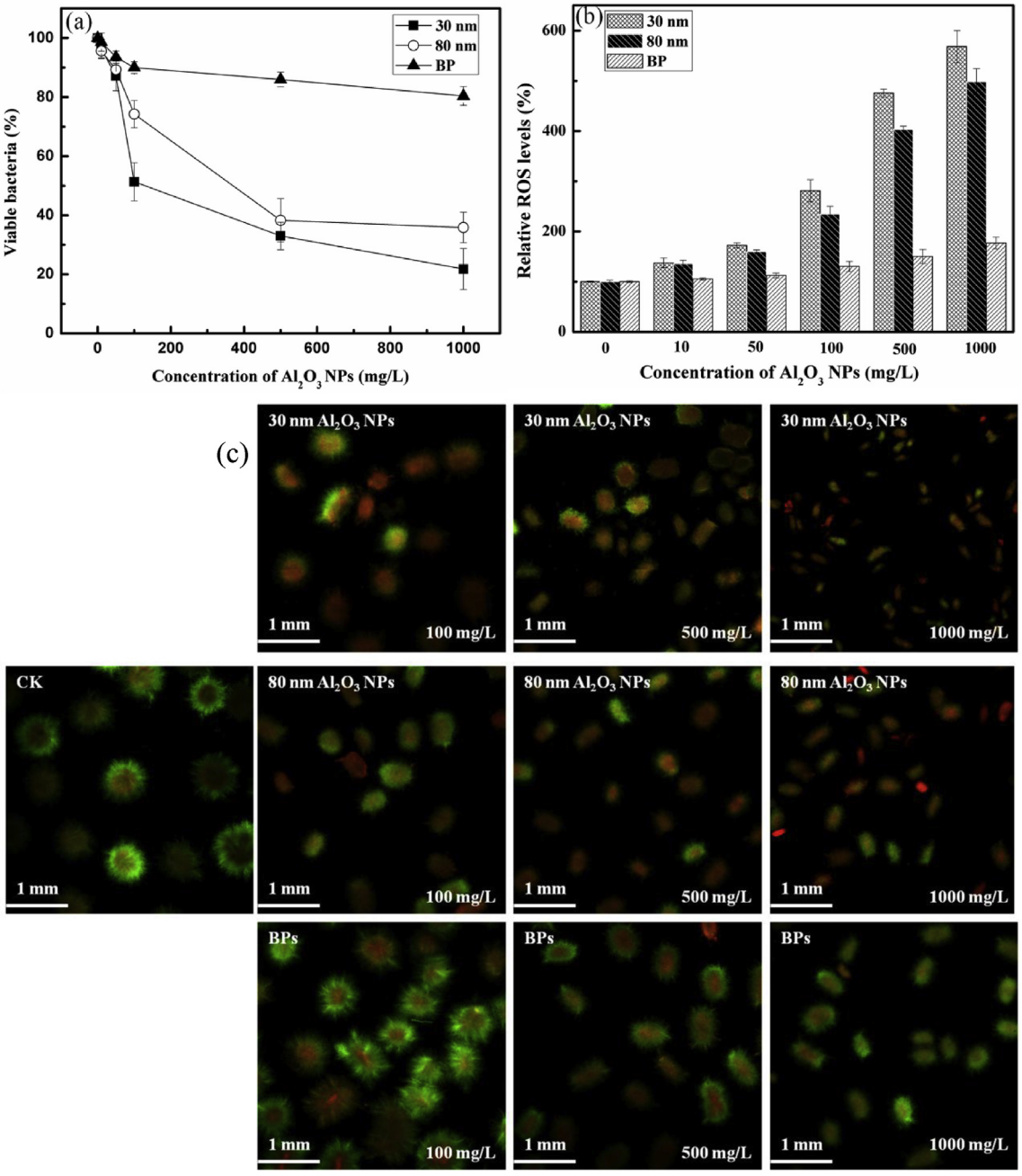

Fig. 1. Toxicity of Al_2O_3 particles to *S. coelicolor* M145 related to variations in size and concentrations in YBP medium after treated for 48 h. The sizes of particles were 30 nm, 80 nm and bulk particles (BP), with the concentration of 0, 10, 50, 100, 500 and 1000 mg/L a: Relative abundances of viable M145 cells exposed to various treatments; b: Intracellular ROS concentrations in M145 cells exposed to various treatments; c: Confocal laser scanning microscopy (CLSM) images of *S. coelicolor* M145 cells after different treatments. CK indicates "control". The scale of each image was 3.9 mm × 3.9 mm, and objective amplification was 10 × .

concentration of 3.7 mg/L was observed after 72 h, which was 3.7-fold greater than that of the control. However, 30 nm Al_2O_3 NPs, had a lesser effect on antibiotic production because the 80 nm Al_2O_3 NPs were less toxic to M145 than the 30 nm Al_2O_3 NPs, and the bacterial survival exposed to 80 nm NPs was higher than that exposed to 30 nm NPs. BPs did not affect the time to produce antibiotics and had little effect on antibiotic yield. The RED concentrations decreased rapidly after 72 h and reached 0.5 mg/L after 120 h under various treatments.

Similarly, ACT production was greatest after exposure to 1000 mg/L of 80 nm Al_2O_3 NPs (Fig. 2b). M145 began to produce ACT at 48 h, and the maximum concentration of approximately 5.0 mg/L was reached after 168 h in 1000 mg/L of 80 nm NPs. There was a significant difference in ACT production between cells exposed to 80 nm and 30 nm NPs at a concentration of 1000 mg/L. Compared with the control, the antibiotics were produced approximately 24 h earlier and the ACT concentration was increased by 4.6-fold.

3.4. Different expression of genes involved in antibiotic production after exposure to Al_2O_3 NPs

Regulation of the production of antibiotics involves complex interactions, and pathway-specific regulators are generally

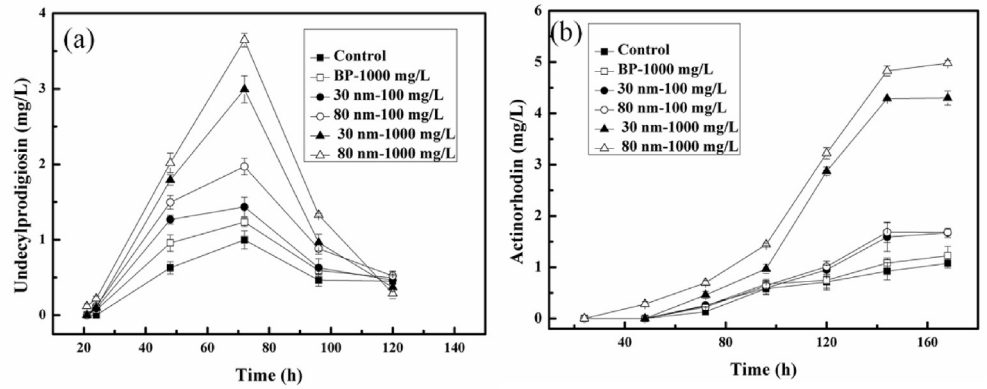

Fig. 2. Time course of antibiotic production in pure cultures of M145 and in cultures of cells exposed to Al_2O_3 particles of 30 nm, 80 nm and bulk particles (BP) with concentrations of 100 and 1000 mg/L for 120–168 h. a: Production of undecylprodigiosin (RED); b: Production of actinorhodin (ACT), Error bar represent standard deviation (n = 3).

considered to have the most direct impact on antibiotic production via transcriptional activation of the relevant biosynthetic genes. In M145, pathway-specific regulatory proteins include RedD/RedZ and ActII-ORF4, which are involved in the biosynthesis of RED and ACT, respectively (Yu et al. 2016). Factors that influence the rates of production and the concentrations of RED and ACT are mostly affected by regulation of transcription or translation of *redD* (SCO5877)/*redZ* (SCO5881) and *actII-ORF4* (SCO5085), respectively (Liu et al. 2013). In this study, the production of the antibiotics and the transcription of *redD*/*redZ* and *actII-ORF4* were significantly increased after exposure to Al_2O_3 NPs (Fig. 3). These changes were the direct cause of the earlier biosynthesis of RED and ACT and the greater ultimate yields. The genes involved in RED production reside in a single cluster (SCO5877 to SCO5898), and the genes involved in ACT production are in another cluster (SCO5071 to SCO5092) (Bentley et al. 2002). The effects of Al_2O_3 NPs on the transcription of these two gene clusters were examined (Fig. 3). Compared to the control, all of the RED-related genes were significantly up-regulated after exposure to Al_2O_3 NPs (Fig. 3a). For ACT, except for SCO5082, SCO5083, SCO5084, SCO5094 (Fig. 3b), all of

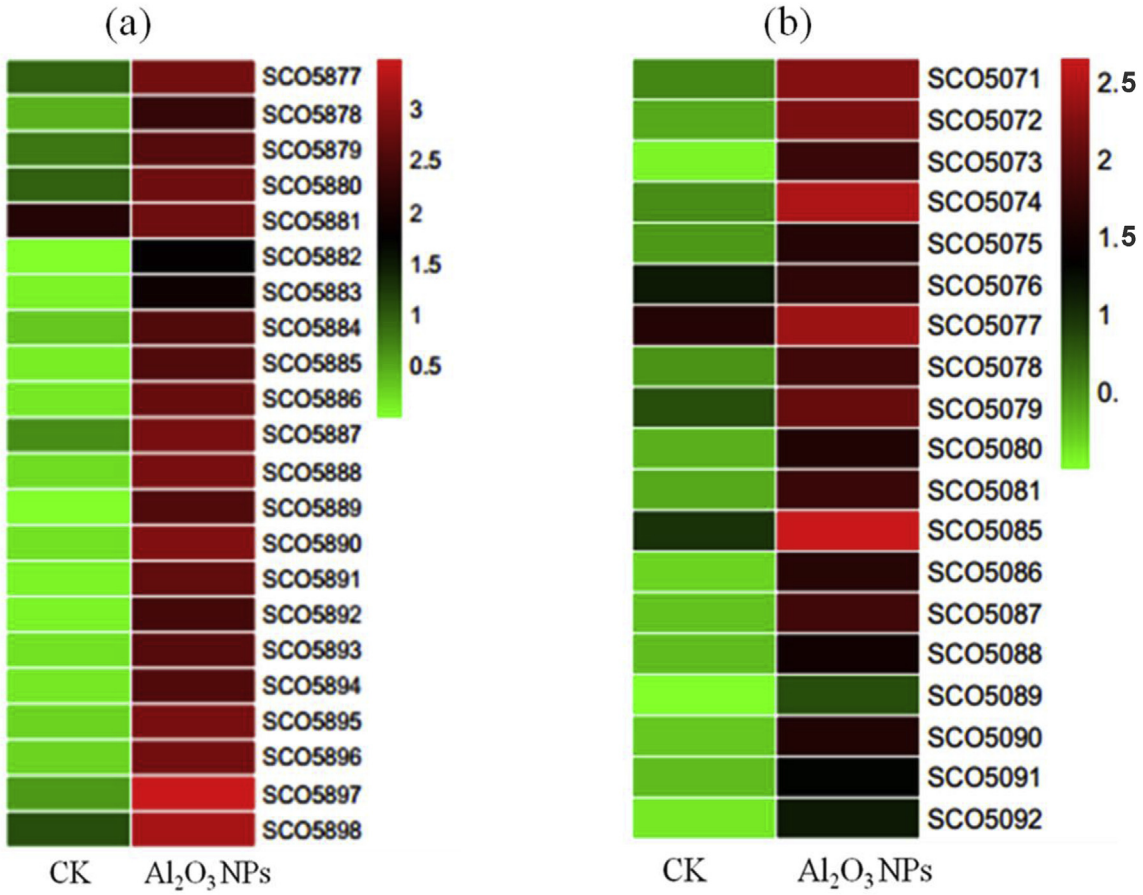

Fig. 3. Gene expression profiles. a: RED; b: ACT. Shown are the relative expression levels of each gene; CK indicates control, Al_2O_3 NPs indicates that the cells were exposed to 1000 mg/L Al_2O_3 NPs (80 nm) for 24 h. (For interpretation of the references to color in this figure legend, the reader is referred to the Web version of this article.)

the other genes were significantly up-regulated after exposure to Al_2O_3 NPs. As an extracellular antibiotic, and consistent with a requirement for export and mechanisms of resistance, the gene cluster associated with ACT production encodes three putative export pumps, actII-ORF2, actII-ORF3, and actVA-ORF1 (Tahlan et al. 2010). The transcription of *actVA-ORF1* (SCO5076), which can export antibiotics to reduce cytotoxicity, was significantly increased after exposure to Al_2O_3 NPs.

To validate the transcriptome data, genes closely related to antibiotic production were quantified by qRT-PCR. Seven genes from the ACT pathway, two genes from the RED pathway, two genes from the two-component system (SCO4229, SCO4230), and one membrane protein gene (SCO2699) were quantified (Table S1), and *S. coelicolor hrdB* was used as the internal control. The fold-changes obtained from the qRT-PCR analysis were consistent with those from the transcriptome experiments (Fig. S3).

3.5. Mechanisms of the effects of Al_2O_3 NPs on S. coelicolor M145

ICP-MS was used to quantify the dissolved Al^{3+} concentrations in suspensions of 100 or 1000 mg/L Al_2O_3 NPs of different sizes (Table S3). The Al^{3+}concentrations under all of the exposure conditions were low, and the morphologies of the M145 cells and the antibiotic production were not affected at these Al^{3+} concentrations. This result indicated that Al^{3+} was not the main cause of the toxicity of Al_2O_3 NPs to M145.

Changes in morphology of M145 cells exposed to 1000 mg/L of 80 nm Al_2O_3 NPs for 48 h were assessed by TEM (Fig. S4). Control cells not exposed to NPs maintained their ellipsoidal shapes (Fig. S3a1, 3b1). In contrast, cells exposed to NPs exhibited significant morphology deformations and were distorted and smaller than the control cells (Fig. S4a2, 4b2). The EDS analysis showed that the Al concentration in the cells treated with Al_2O_3 NPs cells was 0.34%, while the background content was 0.30% for the control cells. The Al concentrations were not significantly different between these two treatments, indicating that Al_2O_3 NPs did not enter the cells (Fig. S5). As the sizes of the NP aggregations reached approximately 800 nm in YBP medium, they were too large to penetrate cells. Therefore, the toxic effect of Al_2O_3 NPs on *Streptomyces* was likely related to the ROS generated from the NPs and the membrane interaction between the cells and the NPs.

Al_2O_3 NPs induced ROS formation in a dose-dependent manner (Fig. 1b). To clarify the roles of ROS in cell death and antibiotic production, the ROS eliminating agent, N-acetylcysteine (NAC), was added one hour before the addition of the nano particles (1000 mg/L, 80 nm). After culturing for 36 h, the ROS concentrations in M145 cells exposed to NPs reached a maximum and then gradually decreased to background levels. After NAC addition, the ROS concentrations were reduced to the level of the controls, indicating that the effects of ROS were substantially eliminated (Fig. 4a). Compared to exposure to Al_2O_3 NPs (1000 mg/L, 80 nm) alone, exposure to NAC resulted in greater survival; however, there was still a discrepancy compared to the control conditions (Fig. 4b). These results suggested that the ROS produced after exposure to Al_2O_3 NPs causes damage to the cells that ultimately results in cell death; however, effects from other factors, such as the direct interaction of nano particles with cell membranes, are possible.

Compared to cells exposed only to Al_2O_3 NPs (1000 mg/L, 80 nm), the RED yield decreased significantly after eliminating intracellular ROS, and time required for RED production was also delayed. RED production was delayed by 3 h after addition of NAC to the medium, compared to production at 21 h when the cells were exposed only to Al_2O_3 NPs. Under the influence of ROS, RED accumulated continuously and reached a maximum level at 72 h. With suppression of ROS in the later period, RED was no longer produced, and it was degraded after cell death during the later period (Fig. 4c). This result indicates that ROS is the main mechanism underlying the stimulation of RED production. ACT production was delayed for 10 h after NAC addition compared to the ACT production at 48 h when the cells were exposed only to Al_2O_3 NPs. There was significantly less ACT produced after NAC addition, indicating that during this stage, ROS played a significant role in promoting

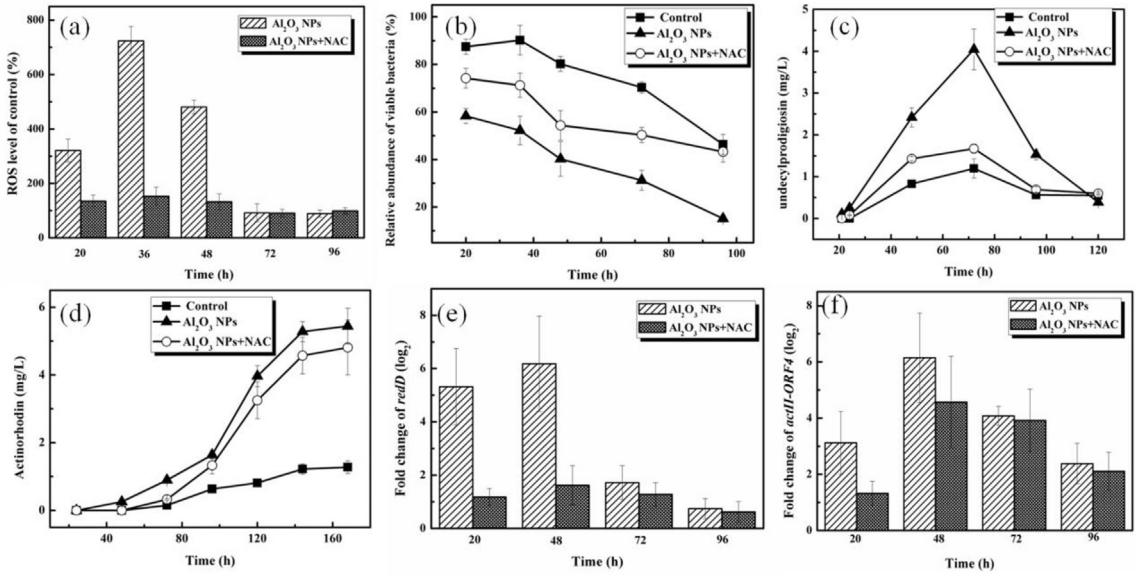

Fig. 4. Role of ROS in Al_2O_3 NP-mediated cell death and antibiotic production. Al_2O_3 NPs in the figure meant M145 cells were treated with 80 nm Al_2O_3 NPs (1000 mg/L); Al_2O_3 NPs + NAC meant M145 cells were treated with a combination of 80 nm Al_2O_3 NPs (1000 mg/L) and 2 mM N-acetylcysteine (NAC). a: ROS levels in M145 cells after treatments for 96 h; b: The relative abundance of viable M145 cells after treatments for 96 h; c: Time course of undecylprodigiosin production after treatments for 120 h and d: actinorhodin production after treatments for 168 h; e: Transcriptional analysis of the *redD* and f: *actII-ORF4* genes after treatments for 96 h. The y-axis shows the fold change in the expression levels in the two experimental groups compared with the control level at each time point, which was set to one.

the production of antibiotics. After the cells were cultured for 72 h, the concentrations of ROS were lower, while the ACT concentration continued to increase until it reached equilibrium after 144 h (Fig. 4d). This result suggested that there were other factors affecting the ACT yield such as the interaction between nano particles and cell membrane.

To assess the effect of NAC supplementation on gene expression, two pathway-specific regulatory genes, *redD* and *actII-ORF4*, which are involved in the biosynthesis of RED and ACT, respectively were chosen for analysis. Compared to cells exposed only to NPs (1000 mg/L, 80 nm), the expression level of *redD* decreased significantly after eliminating intracellular ROS (Fig. 4e). The effect at the transcriptional level confirmed that ROS is likely responsible for the increased RED production. For ACT, compared to the control cells there was no significant difference ($p > 0.05$) in the expression level of *actII-ORF4* after NAC was added at 20 h, indicating that at this point ROS played an important role in improving the expression of the ACT gene. However, after 48 h, there was no significant decrease in the expression level of *actII-ORF4* after eliminating intracellular ROS, confirming that other factors, rather than ROS, affect the expression of the ACT gene during this period (Fig. 4f).

In a previous study, it was found that ROS and NPs were two main factors that affected the growth of *S. coelicolor* (Liu et al. 2018). It was hypothesized that other signals caused by interactions between NPs and cells affected antibiotic production. It has been reported that regulation of secondary metabolism involves not only pathway-specific but also global regulators, many of which are members of two-component systems (TCSs), which is the predominant type of signal transduction system employed by bacteria to monitor and respond to changing environments (Hakenbeck and Stock, 1996). A thorough analysis of the transcriptome indicated that the expression levels of many genes involved in two-component systems were dynamically changed (Table S4, Fig. S6), with some genes being upregulated. Genes such as *vanSB/vanRB* (SCO3589/3590) and *senX3/regX3* (SCO4229/4230) encode sensor kinases that monitor changes outside of the bacterial membranes after NPs were added and response regulators that transfer the signals into the cells. It was possible that the interaction of nanomaterials with membranes enhanced the expression of genes related to two-component systems, which further enhanced the biosynthesis and secretion of antibiotics.

Al_2O_3 NPs inhibited the primary metabolism of *S. coelicolor*. Many genes involved in primary metabolism were downregulated after exposure to NPs; however, the fatty acid metabolic pathway was an exception (Fig. S7). The pathway for the syntheses of fatty acids shares some genes, such as *fabF* and *fabG*, with the pathway for RED synthesis (Sachdeva et al. 2008). Acetyl-CoA is an important substrate for RED and ACT synthesis, so the primary metabolic pathway must have exhibited decreased acetyl-CoA utilization. Various pathways that can generate acetyl-CoA, such as amino acid and fatty acid degradation pathways, were upregulated to ensure the accumulation of antibiotic-expression of genes.

Based on analysis of the transcriptome and the biochemical assays performed in this study, it is proposed that *S. coelicolor* exhibits a complex resistance mechanism to survive in the presence of Al_2O_3 NPs (Fig. 5). Exposure of *S. coelicolor* to 1000 mg/L of Al_2O_3 NPs resulted in enhanced ROS production, which could increase the expression of antibiotic-biosynthesis genes in the period between 0 and 72 h and increase the antibiotic yields. At this stage, many primary metabolic pathways were down-regulated, and *S. coelicolor* focused on the production of antibiotics to resist the hazards of Al_2O_3 NP exposure. During the entire exposure period (0–144 h), the ACT production continued to increase, even with the death of the bacteria after 72 h. This outcome might be due to the effects of the nanomaterials on the membrane surfaces. Nanoparticles continued to affect *Streptomyces*, and cells reacted to the nanomaterials as they would do to harmful microbes; therefore, they elevated the concentration of the extracellular antibiotic ACT to combat the nano particles, and two-component systems played an important role in the process of transferring the extracellular signals into the cells.

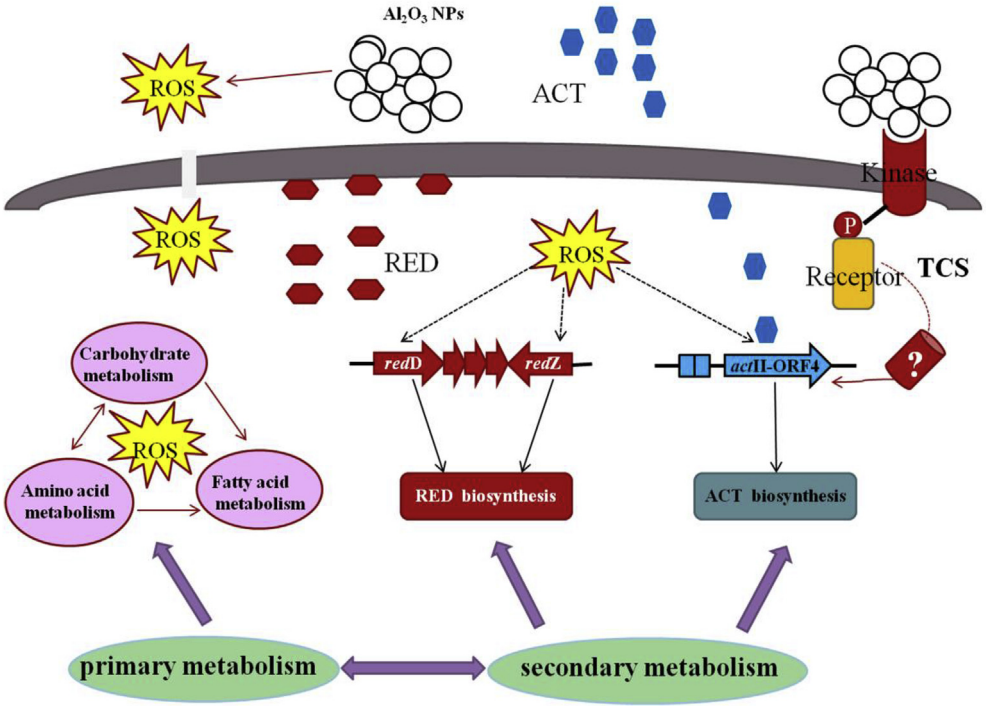

Fig. 5. Model showing how Al_2O_3 NPs affect primary and secondary metabolism in *S. coelicolor* M145.

4. Conclusions

In this study, the effects of Al_2O_3 NPs exposure on *S. coelicolor* growth and antibiotic production were investigated. The toxicity of Al_2O_3 was inversely related to the size of the particles. Compared with NPs, the toxicity of BPs to *S. coelicolor* M145 was much lower. However, compared with 30 nm particles, 80 nm particles improved the secretion of antibiotics and more effectively advanced the initial time of antibiotic production, while BPs had little effect on antibiotic production. The transcriptome data showed significant upregulation of ACT and RED biosynthetic pathways, and this regulation was activated by pathway-specific regulatory proteins. ROS played a crucial role in responding to the effects of the Al_2O_3 NPs on antibiotic production. Our data also suggested a contribution of TCS in this process. Al_2O_3 NPs not only affected secondary metabolic pathways but also inhibited primary metabolism of *S. coelicolor*, which resulted in damage to cell membranes. When cells were attacked by nanomaterials, some primary metabolic pathways were shut down, while others, which were focused on production of secondary metabolites to resist hazards of pollutants, were upregulated. This was the first study explore the toxic effects of Al_2O_3 NPs on cell growth and antibiotic production by *S. coelicolor*.

Declarations of interest

None.

Authors' contributions

JT conceived the idea and designed the experiment, XL performed the experiment and prepared the manuscript. LW analyzed the experimental data, JG revised the article. All authors contributed to the final version.

Acknowledgements

Funding: This work was supported by: (1) National Natural Science Foundation of China [U1806216, 41877372]; (2) Tianjin S&T Program [17PTGCCX00240, 16YFXTSF00520, 17ZXSTXF00050]; and (3) 111 program, Ministry of Education, China [T2017002]. Prof. Giesy was supported by (4) “High Level Foreign Experts” program [#GDT20143200016] funded by the State Administration of Foreign Experts Affairs, the P.R. China to Nanjing University and the Einstein Professor Program of the Chinese Academy of Sciences. He was also supported by the (5) Canada Research Chair program and the (6) Distinguished Visiting Professorship in the School of Biological Sciences of the University of Hong Kong.

Appendix A. Supplementary data

Supplementary data to this article can be found online at https://doi.org/10.1016/j.chemosphere.2019.03.156.

References

Balazs, A.C., Emrick, T., Russell, T.P., 2006. Nanoparticle polymer composites: where two small worlds meet. Science 314, 1107–1110.
Bentley, S.D., Chater, K.F., Challis, G.L., Thomson, N.R., James, K.D., Harris, D.E., Quail, M.A., Kieser, H., Harper, D., 2002. Complete genome sequence of the model actinomycete *Streptomyces coelicolor* A3(2). Nature 417, 141.
Bhatia, S.K., Lee, B.R., Sathiyanarayanan, G., Song, H.S., Kim, J., Jeon, J.M., Kim, J.H., Park, S.H., Yu, J.H., Park, K., 2016. Medium engineering for enhanced production of undecylprodigiosin antibiotic in *Streptomyces coelicolor* using oil palm biomass hydrolysate as a carbon source. Bioresour. Technol. 217, 141–149.
Bhatnagar, A., Kumar, E., Sillanpää, M., 2010. Nitrate removal from water by nano-alumina: characterization and sorption studies. Chem. Eng. J. 163, 317–323.
Binh, C.T., Tong, T., Gaillard, J.F., Gray, K.A., Kelly, J.J., 2014. Acute effects of TiO_2 nanomaterials on the viability and taxonomic composition of aquatic bacterial communities assessed via high-throughput screening and next generation sequencing. PLoS One 9, e106280.
Borodina, I., Siebring, J., Zhang, J., Smith, C.P., Van, K.G., Dijkhuizen, L., Nielsen, J., 2008. Antibiotic overproduction in *Streptomyces coelicolor* A3(2) mediated by phosphofructokinase deletion. J. Biol. Chem. 283, 25186–25199.
Cerdeño, A.M., Bibb, M.J., Challis, G.L., 2001. Analysis of the prodiginine biosynthesis gene cluster of *Streptomyces coelicolor* A3(2): new mechanisms for chain initiation and termination in modular multienzymes. Chem. Biol. 8, 817–829.
Dinesh, R., Anandaraj, M., Srinivasan, V., Hamza, S., 2012. Engineered nanoparticles in the soil and their potential implications to microbial activity. Geoderma 173–174, 19–27.
Ding, C., Pan, J., Jin, M., Yang, D., Shen, Z., Wang, J., Zhang, B., Liu, W., Fu, J., Guo, X., 2016. Enhanced uptake of antibiotic resistance genes in the presence of nano-alumina. Nanotoxicology 10, 1051–1060.
Eduok, S., Martin, B., Villa, R., Nocker, A., Jefferson, B., Coulon, F., 2013. Evaluation of engineered nanoparticle toxic effect on wastewater microorganisms: current status and challenges. Ecotoxicol. Environ. Saf. 95, 1–9.
Ganguly, P., Poole, W.J., 2003. In situ measurement of reinforcement stress in an aluminum–alumina metal matrix composite under compressive loading. Mater. Sci. Eng., A 352, 46–54.
Gottelt, M., Kol, S., Gomezescribano, J.P., Bibb, M., Takano, E., 2010. Deletion of a regulatory gene within the cpk gene cluster reveals novel antibacterial activity in *Streptomyces coelicolor* A3(2). Microbiology 156, 2343–2353.
Hakenbeck, R., Stock, J.B., 1996. Analysis of two-component signal transduction systems involved in transcriptional regulation. Methods Enzymol. 273, 281–300.
Hesketh, A., Chen, W., Ryding, J., Chang, S., Bibb, M., 2007. The global role of ppGpp synthesis in morphological differentiation and antibiotic production in *Streptomyces coelicolor* A3(2). Genome Biol. 8, 1–18.
Hindra, Pak, P., Elliot, M.A., 2010. Regulation of a novel gene cluster involved in secondary metabolite production in *Streptomyces coelicolor*. J. Bacteriol. 192, 4973.
Huang, B., Liu, N., Rong, X., Ruan, J., Huang, Y., 2015. Effects of simulated microgravity and spaceflight on morphological differentiation and secondary metabolism of *Streptomyces coelicolor* A3(2). Appl. Microbiol. Biotechnol. 99, 4409–4422.
Jiang, W., Mashayekhi, H., Xing, B., 2009. Bacterial toxicity comparison between nano- and micro-scaled oxide particles. Environ. Pollut. 157, 1619–1625.
Kamnev, A.A., 2008. FTIR spectroscopic studies of bacterial cellular responses to environmental factors, plant-bacterial interactions and signalling. Spectroscopy 22, 83–95.
Kaweeteerawat, C., Ivask, A., Liu, R., Zhang, H., Chang, C.H., Low-Kam, C., Fischer, H., Ji, Z., Pokhrel, S., Cohen, Y., 2015. Toxicity of metal oxide nanoparticles in *Escherichia coli* correlates with conduction band and hydration energies. Environ. Sci. Technol. 49, 1105–1112.
Kim, M., Yi, J.S., Lakshmanan, M., Lee, D.Y., Kim, B.G., 2016. Transcriptomics-based strain optimization tool for designing secondary metabolite overproducing strains of *Streptomyces coelicolor*. Biotechnol. Bioeng. 113, 651–660.
Lee, J., Mahendra, S., Alvarez, P.J., 2010. Nanomaterials in the construction industry: a review of their applications and environmental health and safety considerations. ACS Nano 4, 3580–3590.
Li, J., Zhou, H., Wang, J., Wang, D., Shen, R., Zhang, X., Jin, P., Liu, X., 2016. Oxidative stress-mediated selective antimicrobial ability of nano-VO_2 against Gram-positive bacteria for environmental and biomedical applications. Nanoscale 8, 11907–11923.
Liu, G., Chater, K.F., Chandra, G., Niu, G., Tan, H., 2013. Molecular regulation of antibiotic biosynthesis in streptomyces. Microbiol. Mol. Biol. Rev. 77, 112–143.
Liu, X., Tang, J., Wang, L., Giesy, J.P., 2018. Mechanisms of oxidative stress caused by CuO nanoparticles to membranes of the bacterium *Streptomyces coelicolor* M145. Ecotoxicol. Environ. Saf. 158, 123–130.
Martınez-Flores, E., Negrete, J., Villaseñor, G.T., 2003. Structure and properties of Zn–Al–Cu alloy reinforced with alumina particles. Mater. Des. 24, 281–286.
Mu, D., Xin, M., Xu, Z., Du, Z., Chen, G., 2015. Removing *Bacillus subtilis* from fermentation broth using alumina nanoparticles. Bioresour. Technol. 197, 508–511.
Oberdorster, G.O.E., Oberdorster, J., 2005. Nanotoxicology: an emerging discipline evolving from studies of ultrafine particles. Environ. Health Perspect. 113, 823–839.
Pakrashi, S., Dalai, S., Sabat, D., Singh, S., Chandrasekaran, N., Mukherjee, A., 2011. Cytotoxicity of Al_2O_3 nanoparticles at low exposure levels to a freshwater bacterial isolate. Chem. Res. Toxicol. 24, 1899.
Papireddy, K., Smilkstein, M., Kelly, J.X., Shweta, Salem, S.M., Alhamadsheh, M., Haynes, S.W., Challis, G.L., Reynolds, K.A., 2011. Antimalarial activity of natural and synthetic prodiginines. J. Med. Chem. 54, 5296–5306.
Patkari, M., Mehra, S., 2013. Transcriptomic study of ciprofloxacin resistance in *Streptomyces coelicolor* A3(2). Mol. Biosyst. 9, 3101–3116.
Qiu, Z., Yu, Y., Chen, Z., Jin, M., Yang, D., Zhao, Z., Wang, J., Shen, Z., Wang, X., Qian, D., 2012. Nanoalumina promotes the horizontal transfer of multiresistance genes mediated by plasmids across genera. P. Natl. Acad. Sci. USA 109, 4944–4949.
Robichaud, C.O., Uyar, A.E., Darby, M.R., Zucker, L.G., Wiesner, M.R., 2009. Estimates of upper bounds and trends in nano-TiO_2 production as a basis for exposure assessment. Environ. Sci. Technol. 43, 4227–4233.
Sigle, S., Steblau, N., Wohlleben, W., 2016. Polydiglycosylphosphate transferase PdtA

(SCO2578) of *Streptomyces coelicolor* A3(2) is crucial for proper sporulation and apical tip extension under stress conditions. Appl. Environ. Microbiol. 82, 5661.
Sachdeva, S., Musayev, F.N., Alhamadsheh, M.M., Scarsdale, J.N., Wright, H.T., Reynolds, K.A., 2008. Separate entrance and exit portals for ligand traffic in mycobacterium tuberculosis FabH. Chem. Biol. 15, 402–412.
Sadiq, I.M., Chowdhury, B., Chandrasekaran, N., Mukherjee, A., 2009. Antimicrobial sensitivity of *Escherichia coli* to alumina nanoparticles. Nanomed. Nanotechnol. 5, 282–286.
Schäberle, T.F., Orland, A., König, G.M., 2014. Enhanced production of undecylprodigiosin in *Streptomyces coelicolor* by co-cultivation with the corallopyronin A-producing myxobacterium, *Corallococcus coralloides*. Biotechnol. Lett. 36, 641–648.
Schaumann, G.E., Philippe, A., Bundschuh, M., Metreveli, G., Klitzke, S., Rakcheev, D., Grün, A., Kumahor, S.K., Kühn, M., Baumann, T., 2015. Understanding the fate and biological effects of Ag- and TiO_2-nanoparticles in the environment: the quest for advanced analytics and interdisciplinary concepts. Sci. Total Environ. 535, 3–19.
Simon-Deckers, A., Loo, S., Mayne-L'Hermite, M., Herlin-Boime, N., Menguy, N., Reynaud, C., Gouget, B., Carrière, M., 2009. Size-, composition- and shape-dependent toxicological impact of metal oxide nanoparticles and carbon nanotubes toward bacteria. Environ. Sci. Technol. 43, 8423.
Taguchi, T., Yabe, M., Odaki, H., Shinozaki, M., Metsä-Ketelä, M., Arai, T., Okamoto, S., Ichinose, K., 2013. Biosynthetic conclusions from the functional dissection of oxygenases for biosynthesis of actinorhodin and related Streptomyces antibiotics. Chem. Biol. 20, 510–520.
Tahlan, K., Ahn, S.K., Sing, A., Bodnaruk, T.D., Willems, A.R., Davidson, A.R., Nodwell, J.R., 2010. Initiation of actinorhodin export in *Streptomyces coelicolor*. Mol. Microbiol. 63, 951–961.
van Wezel, G.P., White, J., Hoogvliet, G., Bibb, M.J., 2000. Application of redD, the transcriptional activator gene of the undecylprodigiosin biosynthetic pathway, as a reporter for transcriptional activity in *Streptomyces coelicolor* A3(2) and *Streptomyces lividans*. J. Mol. Microbiol. Biotechnol. 2, 551–556.
Williamson, N.R., Fineran, P.C., Leeper, F.J., Salmond, G.P., 2006. The biosynthesis and regulation of bacterial prodiginines. Nat. Rev. Microbiol. 4, 887–899.
Xu, Y., Willems, A., Au-Yeung, C., Tahlan, K., Nodwell, J.R., 2012. A two-step mechanism for the activation of actinorhodin export and resistance in *Streptomyces coelicolor*. MBio 3, 00191-00112.
Yang, Y.H., Joo, H.S., Lee, K., Liou, K.K., Lee, H.C., Sohng, J.K., Kim, B.G., 2005. Novel method for detection of butanolides in *Streptomyces coelicolor* culture broth, using a His-tagged receptor (ScbR) and mass spectrometry. Appl. Environ. Microbiol. 71, 5050–5055.
Yu, L., Gao, W., Li, S., Pan, Y., Liu, G., 2016. A GntR family regulator SCO6256 is involved in antibiotic production and conditionally regulates the transcription of myo-inositol catabolic genes in *Streptomyces coelicolor* A3(2). Microbiology 162, 537.

Al_2O_3 nanoparticles promote secretion of antibiotics in *Streptomyces coelicolor* by regulating gene expression through the nano effect

Xiaomei Liu[a], Jingchun Tang[a]*, Lan Wang[a], John P. Giesy[b,c]

[a]Key Laboratory of Pollution Processes and Environmental Criteria (Ministry of Education), Tianjin Engineering Research Center of Environmental Diagnosis and Contamination Remediation, College of Environmental Science and Engineering, Nankai University, Tianjin 300350, China.

[b] Toxicology Centre, University of Saskatchewan, Saskatoon, Saskatchewan, Canada

[c]Department of Veterinary Biomedical Sciences, University of Saskatchewan, Saskatoon, Saskatchewan, Canada

*Corresponding author: E-mail: tangjch@nankai.edu.cn; Tel: +86-13682055616.

Materials and Methods

Analysis of concentrations of Al^{3+} in media

To estimate dissolution of Al_2O_3 in the media, the Al^{3+} concentrations were determined after shaking for 48 h at concentrations of 100 or 1000 mg/L Al_2O_3. The suspensions were centrifuged at 10,000 ×g for 20 min, and then the supernatant was filtered twice through 0.22 μm membranes. The Al^{3+} concentration was quantified by inductively coupled plasma mass spectrometry (ICP-MS) (Elan drc-e, Perkin Elmer, America).

TEM

The intracellular effects of NPs were assessed by transmission electron microscopy (TEM) (HT7700, Hitachi, Beijing, China) and energy dispersive X-ray spectroscopy (EDS) at the Tianjin Institute of Industrial Biotechnology, Chinese Academy of Sciences. After treatment with Al_2O_3 NPs (80 nm, 1000 mg/ L) for 48 h, the cell pellets were centrifuged at 4,000 ×g for 10 min and then fixed with 2.5% glutaraldehyde in 0.1 M phosphate buffer (PBS, pH 7.2). After fixation, the samples were treated with 1% osmium tetroxide for 1 h. Next, the pellets were dehydrated in a series of solutions with increasing ethanol concentrations (30, 50, 70, 80 and 90%, for 15 min each), rinsed in acetone three times for 20 min at room temperature, and then embedded in resin. The resin blocks were sectioned using an ultramicrotome (Leica EM UC7, Solms, Germany) with a diamond knife. The ultra-thin sections were stained with uranyl acetate (2%, 20 min, 25°C) for TEM observation.

Quantitative real-time PCR (qRT-PCR)

Quantitative real-time PCR (qRT-PCR) analysis of genes closely related to antibiotic production was performed based on the previously described methods (Zhang *et al.* 2017). The primers used are listed in Table S1, and the quantification was performed on a Roche Light Cycler 480 thermal cycler (Roche, Basel, Switzerland) with SYBR *Premix Ex Taq* (TaKaRa). The reactions were carried out under the following conditions: 95°C for 1 min followed by 40 cycles of 95°C for 5 s, 60°C for 20 s and 72°C for 30 s. PCR analyses were performed in triplicate for each transcript, and the *hrdB* gene (Gottelt *et al*. 2010), which encodes the major sigma factor of *Streptomyces,* was used as an internal control.

Results

Table S1 List of primers used for quantitative RT-PCR

Gene	Name		Primer sequence
SCO5071	*actⅥ-A*	F	CGGCCACCAGATGCAGAA
		R	TTGCGGGCGTCGAACTTGC
SCO5072	*actⅥ-1*	F	CACGCCCTCGTGCTGTCCT
		R	CGATGTGCGGTGGGTTGAA
SCO5082	*actⅡ-1*	F	CGGTCGCTGCGGAGGATGTT
		R	TAGGCGGCGAGTTCGTCGTG
SCO5083	*actⅡ-2*	F	GGCTGGGCGACATCTACGG
		R	TGGGCGGGAACATTTGCT
SCO5085	*actⅡ-ORF4*	F	CCTGGTGCTGCTGCTCCTCA
		R	ATTCCCGGTCGTCGCTCGTC
SCO5086	*actⅢ*	F	GAAGAAGGACTGCGGACGACG
		R	GACCGTAACGCTCGACCACC
SCO5087	*actⅠ*	F	GACGATGACGACGACCACCGGACGAA
		R	CCCGAGGTGAGCAGTTCCCAGAA
SCO5877	*redD*	F	GGACCTGGTGGACGAACTGTGGG
		R	AGTCTCAGGAAGCGGTTGCCGTC
SCO5881	*redZ*	F	ACCCGTGTCCTGGTGTGCTGCGA
		R	CTTGCCGAGTCGTGCGAGTTCCG
SCO5820	*hrdB*	F	GGGCTACAAGTTCTCCACG
		R	AGGTCCTGGAGCATCTGGC
SCO4229	*senX3*	F	AGTACTCACCGGCGTCATCG
		R	CACGGGATCGGTGTGGAGCG
SCO4230	*regX3*	F	TGGTGACCGCCAAGGACAGC
		R	TACGGCTCGGATGCGGGCGA
SCO2699		F	GTGTCCTGTCCGGCAACGTCGTC
		R	GCCGTAGCCGCCGCTCTTGTCGT

Table S2. Characterization of various sizes of Al_2O_3 (n=10)

	30 nm	80 nm	BPs
Particle size	34.5±1.5 nm	88.4±5.8nm	5.62±0.57 μm
DLS	827±33 nm	871±41 nm	5.73±0.69 μm

Table S3. Concentrations of Al^{3+} in various sizes of of NPs (30 and 80 nm) and BPs and different concentration (100 mg/L and 1000 mg/L) Al_2O_3 NPs in YBP medium.

	100 mg/L (mg/L)	1000 mg/L (mg/L)
30 nm	2.18±0.11	10.58±0.38
80 nm	1.34±0.05	6.21±0.46
BPs	0.62±0.02	1.18±0.03

Table S4: List of genes involved in two-component system that were up-regulated.

Gene ID	Gene name	Biological role	Fold change (log_2C)
SCO0382	*algD*	GDP-mannose dehydrogenase	7.7
SCO1290	*phoD*	alkaline phosphatase	7.6
SCO1613	*glnA*	glutamine synthetase	2.0
SCO2068	*phoD*	alkaline phosphatase	5.5
SCO2286	*phoD*	alkaline phosphatase	10.2
SCO3079	*atoB*	acetyl-CoA acetyltransferase	1.7
SCO3589	*vanSB*	two component sensor kinase	2.3
SCO3590	*vanRB*	two-component system response regulator	1.7
SCO4142	*pstS*	phosphate-binding protein	7.5
SCO4229	*senX3*	sensor kinase	3.3
SCO4230	*regX3*	response regulator	3.5
SCO4947	*narG*	nitrate reductase A subunit alpha	6.8
SCO4948	*narH*	nitrate reductase	9.5
SCO4949	*narJ*	nitrate reductase subunit delta NarJ3	7.9
SCO4950	*narG*	nitrate reductase subunit gamma NarI3	6.5
SCO5399	*atoB*	acetyl-CoA acetyltransferase	1.9
SCO5584	*glnB*	nitrogen regulatory protein P-II	2.2
SCO5585	*glnD*	uridylyltransferase	2.9
SCO6685	*desR*	transcriptional regulator	2.1
SCO6731	*atoB*	acetyl-CoA acetyltransferase	1.7
SCO6816	*pstS*	ABC transporter	4.9
SCO6962	*glnA*	glutamine synthetase	2.0
SCO7534	*mtrB*	histidine kinase	1.7

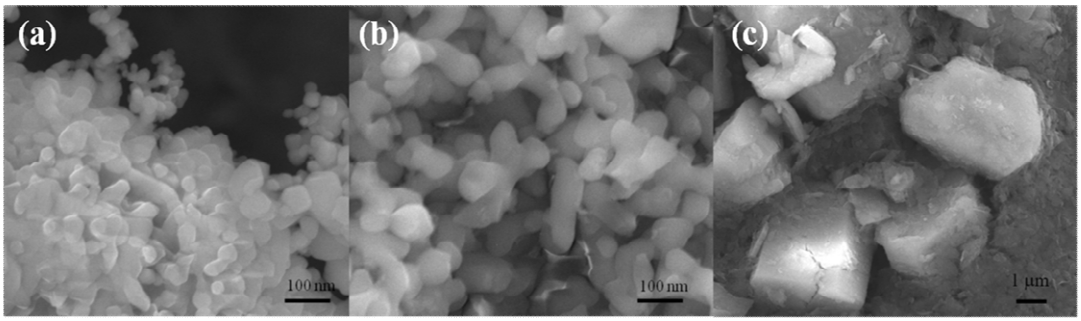

Figure S1: The SEM images of Al_2O_3 particles of various sizes. a: 30 nm; b: 80 nm; c: Bulk particles.

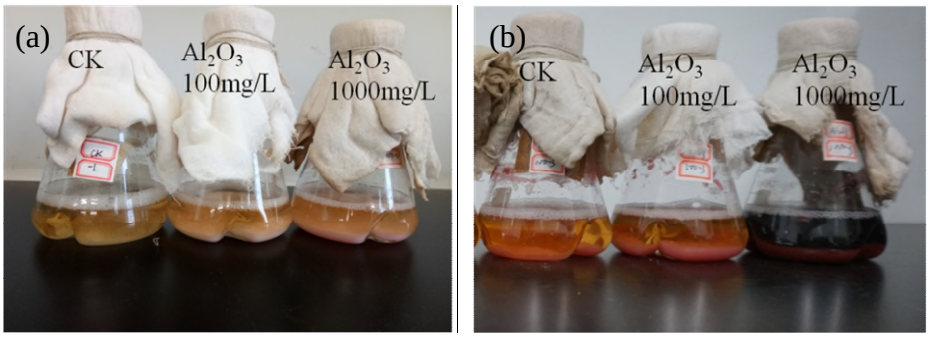

Figure S2: Time course of production of antibiotics in pure culture of *S. coelicolor* and that interacted with Al_2O_3 particles. a: Production of antibiotics in pure culture of *S. coelicolor* and that exposed for 21 h to Al_2O_3 particles; b: picture of production of antibiotics in pure culture of *S. coelicolor* and that exposed for 48 h to Al_2O_3 particles.

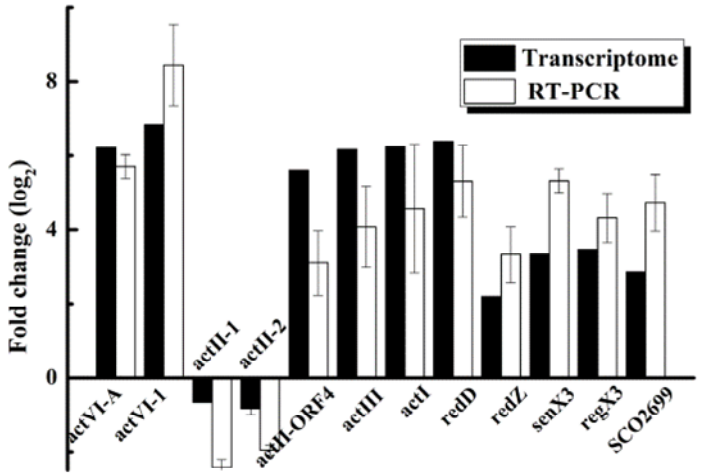

Figure S3: Validation of transcriptome data by use of quantitative RT-PCR. The fold changes of genes from various functional passways were determined by quantitative RT-PCR and the transcriptome. Negative fold changes implied down regulation of genes after exposure to Al_2O_3 NPs.

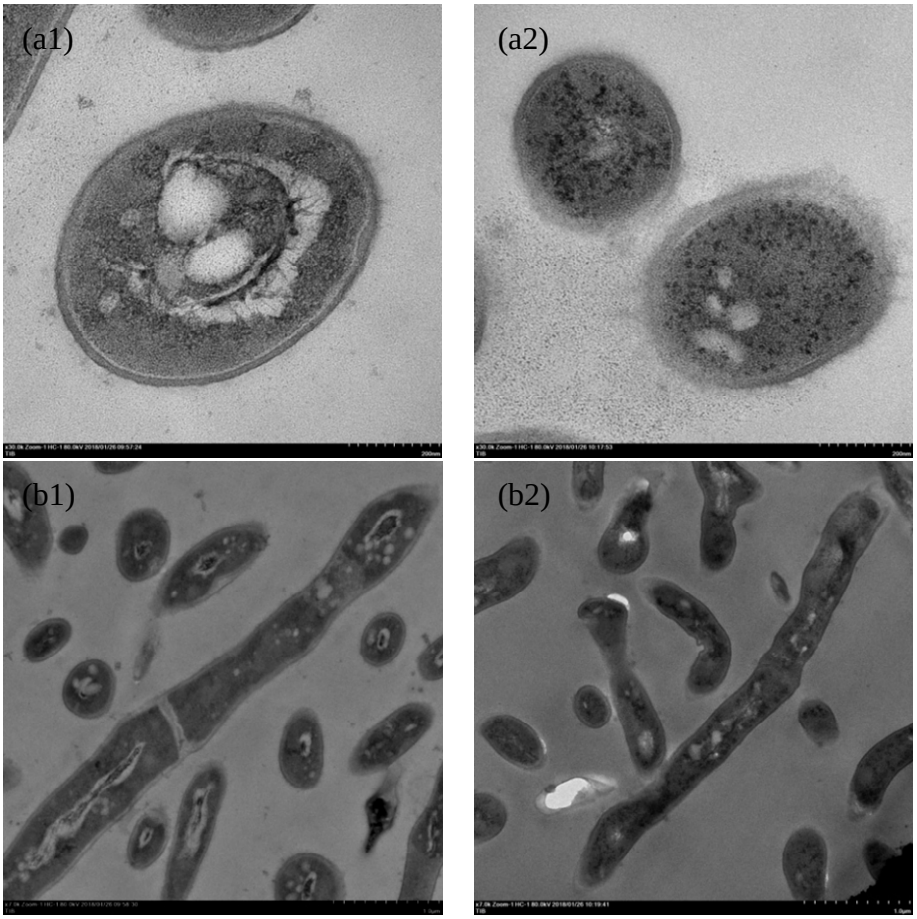

Figure S4: TEM imaging of changes in morphology of M145 after exposure to 80 nm Al_2O_3 NPs at 100 mg/L for 48 h. a: the images×20000, a1: the control not exposed to NP, a2: M145 exposed to NP; b: the images×7000, b1: the control not exposed to NP, b2: M145 exposed to NP.

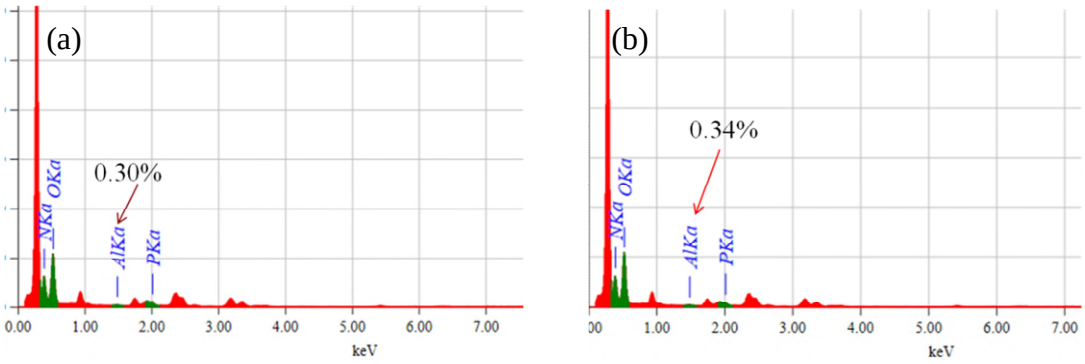

Figure S5: Aluminum (Al) content in cells quantified by use of EDX, a:control without exposure to NP, b: *S. coelicolor* M145 exposed to NPs

Figure S6: Profiles of expression of genes by a two-component system. Displayed are relative expressions of each gene. CK means control, Al_2O_3 NPs means exposed to 1000 mg/L Al_2O_3 NPs. Color indications are red for increased expression, green for decreased expression and black for unchanged expression.

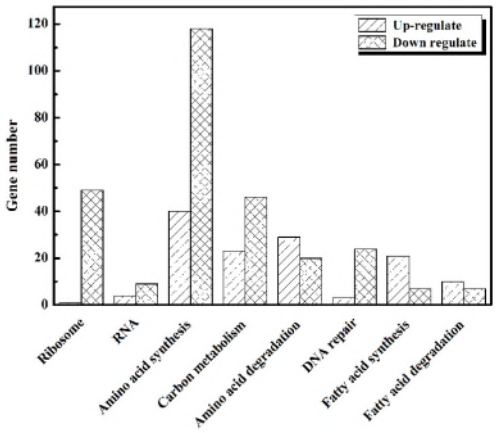

Figure S7: Changes in expressions of genes related to primary metabolic pathways.